

Most of the key issues in the previous version of the MS have been addressed. The inclusion of size-resolved AMS chemical composition in particular makes the paper much more valuable. The conclusions are interesting and provide new insights. I recommend publication after the corrections below are made.

\*\*\*\*\*

Thanks for reviewing the manuscript again. We made all corrections in the revised manuscript.

\*\*\*\*\*

Corrections:

Page 3, Line 24: Throughout the text of the MS, the device to measure number size distributions is called Twin Differential Mobility Particle Sizer (TDMPS), but in table 1 it is called SMPS.

**Response:**

“SMPS” in the table 1 was replaced by “TDMPS”.

**Modification in the MS:**

Table 1: The summary of instruments and parameters used in this study.

Instrument	Parameter
TDMPS	Particle number size distribution
HTDMA	Particle hygroscopicity
HR-ToF-AMS	Size-resolved chemical composition
Monitor – APSA 360 Horiba Europe	SO <sub>2</sub> concentration
Kipp & Zonen CM6 Pyranometer	Global solar irradiance

\*\*\*\*\*

Page 4 Line 8: Please clarify whether this is meant to say that scans with RH between 87% and 93% (3% in either direction) were accepted, or whether the acceptable range was 88.5% – 91.5% (3% symmetrically around the setpoint).

**Response:**

The data with RH between 87% and 93% were accepted. It will be clarified in the revised manuscript.

**Modification in the MS:**

“Hygroscopicity measurements with RH between 87% and 90% were accepted for further analysis.”

\*\*\*\*\*

Page 9, Line 11: “mean geometric diameter” should be “geometric mean diameter”

**Response:**

The “mean geometric diameter” was replaced by “geometric mean diameter” in the revised manuscript.

**Modification in the MS:**

“where D<sub>m</sub> is a geometric mean diameter of log-normal ultrafine particle mode, which has been fitted to the number size distribution”

\*\*\*\*\*

Page 12, Line 13: “decreased to 10 C” – This reads as if a fast decrease in T to 10C were observed. It would be better to write “decreased to an eventual nighttime minimum of around 10 C”

**Response:**

It was corrected in the manuscript.

**Modification in the MS:**

“Simultaneously, ambient temperature decreased to an eventual nighttime minimum of around 10°C.”

\*\*\*\*\*

Page 14, Line 13: “Here we assume that the weather condition and boundary layer height were similar during two time periods (see meteorological parameters in Fig. 3). Therefore, the effect of boundary layer dynamics on the change in CCN number concentration could be ignored”: The second sentence should be worded more carefully, such as “Therefore we assumed that .....could be ignored.”, because there is still no guarantee that BL effects were indeed absent.

**Response:**

The sentence was modified in the manuscript.

**Modification in the MS:**

“Therefore, we assumed that the effect of boundary layer dynamics on the change in CCN number concentration could be ignored.”

\*\*\*\*\*

Figure 1: The contour plot still has a linear scale on the concentration, which leads to fast saturation of the plot in both the low and the high concentration range and considerable loss of information on the shape of the size distribution. A logarithmic concentration scale would work better. What is the unit and axis for H<sub>2</sub>SO<sub>4</sub>? Please note the meaning of the black dashed lines in the contour plot in the caption.

**Response:**

The log scale for Z value was taken in the contour plot. In the panel (b), the particle number concentration and H<sub>2</sub>SO<sub>4</sub> concentration have the same y axis and the unit. The black dashed lines in panel (a) indicate the particles diameters of 35, 50, and 75 nm. These are clarified in the revised manuscript.

**Modification in the MS:**

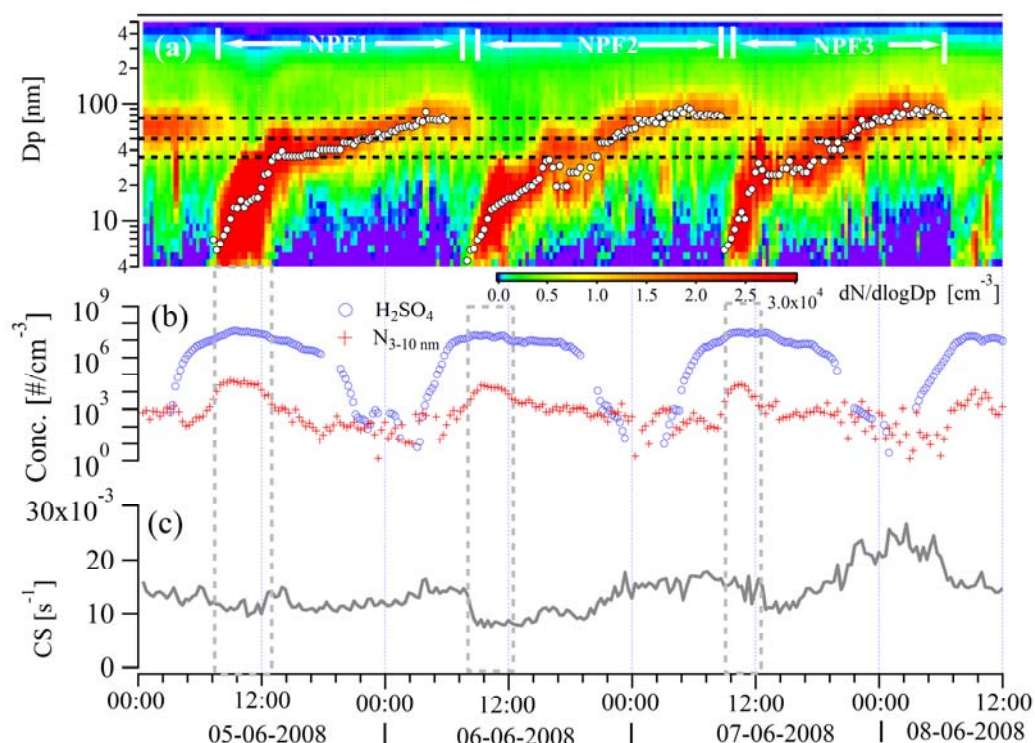


Fig. 1: Particle number size distribution (a), 3-10 nm particle number concentration and  $\text{H}_2\text{SO}_4$  concentration (b), condensation sink (CS) (c) during the NPF events. The starting and ending time of the events were marked in the upper place of panel (a) by NPF1, NPF2, and NPF3. The while circles in the panel (a) are the  $D_m$  of new particles modes. The grey dashed lines indicated the time period of particle formation. The black dashed lines in panel (a) indicate the particle sizes of 35, 50, and 75 nm. In the panel (b), the particle number concentration and  $\text{H}_2\text{SO}_4$  concentration share the same y axis and the unit.

\*\*\*\*\*

Figure 2: The axis for wind speed is labeled wrong. It would be nice if the beginning and end of the NPF events were marked in this plot, too.

**Response:**

The label “wind speed [m/s]” was corrected.

**Modification in the MS:**

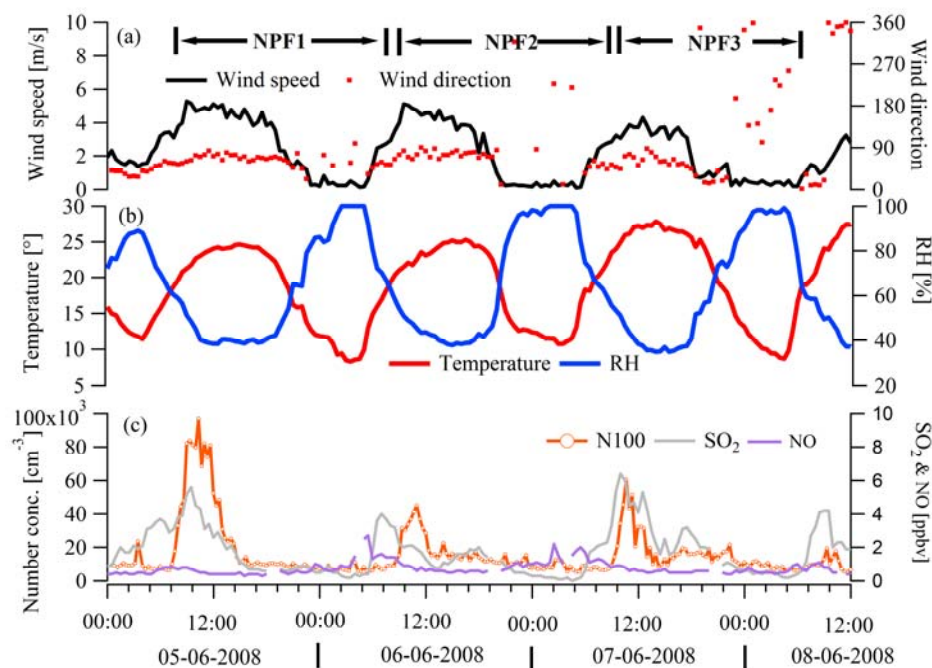


Fig. 2: The time series of wind speed and wind direction (a), ambient temperature and RH (b), and SO<sub>2</sub> & NO concentrations and number concentrations of particles in diameters of 3-100 nm (b). The starting and ending time of the events were marked in the upper place of panel (a) by NPF1, NPF2, and NPF3.

\*\*\*\*\*

Figure 3: Please mark the particle formation periods (see also comment below).

**Response:**

The particle formation periods were marked in the revised plot.

**Modification in the MS:**

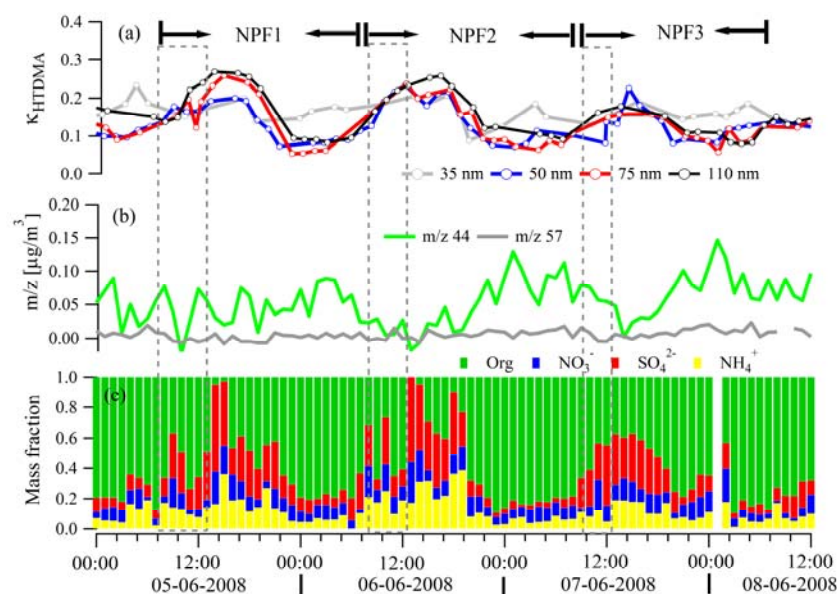


Fig.3: Size-resolved particle hygroscopicity (a), m/z 44 and 57 mass concentrations in 30-100 nm particles (b), and mass fraction of organic, sulfate, nitrate, and ammonium in 30-100 nm particles (c). The grey dashed lines indicated the time period of particle formation.

\*\*\*\*\*

The paper should go through another English edit, as language errors sometimes interfere with the understanding of the content. The most critical error is this one: Page 1, Line 19, page 13, line 5, and page 16, line 2: “were dominated” – this should probably read “dominated”: if I understand the authors correctly from the context, they mean to say that sulfate and ammonium made up the major fraction of chemical components in those instances. “Were dominated”, however, means that some other chemical species is more important (“dominated by what?”). Together with the fact that it is not entirely obvious which time frame in Figure 3 this repeating statement refers to, this leaves the reader guessing. Moreover, based on the other plots, it is not completely clear that sulfate and ammonium were indeed the dominating species in the particle formation period.

**Response:**

We tried our best to improve the English writing. Thanks for pointing out misapplication of “dominated”. We took a closer look at Fig. 3 and found that the sulfate and ammonium are not dominating species in the particle formation period. Actually, the particles are dominated by organic compounds in this period. In the revised manuscript, we corrected this mistake.

**Modification in the MS:**

As displayed in Fig.3 (c), the organic compounds were dominating species in 30-100 nm particles in the particle formation period (indicated by grey dashed line). In this period, most of newly formed particles were smaller than 30 nm, as shown in Fig. 1 (a). They are too small to be detected by HR-ToF-AMS. Therefore, AMS measurements cannot provide proper information on chemical composition of newly formed particles in particle formation period. After around 12:00, the newly formed particles grew beyond 30 nm. Simultaneously, an obvious increase in sulfate and ammonium mass fraction in 30-100 nm particles was observed. This indicates that the newly formed particles were dominated by sulfate and ammonium.

\*\*\*\*\*

There are multiple other language errors, including, but not limited to:  
Use of the word “potential”: Page 2, Line 7: what are “potential CCN”? The insecurity in the statement is sufficiently stated by the word “possibly”;

**Response:**

The word “potential” was deleted from the text.

**Modification in the MS:**

This new particle formation (NPF) process represents an important source of

atmospheric particles and possibly also for the number concentration of cloud condensation nuclei (CCN)

\*\*\*\*\*

Page 13, Line 3: “were major potential contributors to the particle growth” – better: “were potentially major contributors...”

**Response:**

It was corrected in the revised MS.

**Modification in the MS:**

Both particle hygroscopicity measurements and numerical analysis showed that organics were potentially major contributors to the particle growth.

\*\*\*\*\*

Page 5, Line 15: “The detail description about the calculation was given...”

**Response:**

It was corrected in the revised MS.

**Modification in the MS:**

The detail description can be found in Poulain et al. (2014).

\*\*\*\*\*

Page 6 , Line 3: “e.g.” should be “i.e.”

Page 7, Line 19: “This reason was given as follow” – “The reason is given as follows”

Page 8, Line 13: “is referred to represent” should be “refers to”

Page 10, Line 24; “grew versus time” – “grew with time”

Page 10, line 25: “refere”

**Response:**

These mistakes were corrected in the revised MS.

\*\*\*\*\*

Page 11, Line 13: “cities away tens of kilometers from the station via transportation”;

**Response:**

It was corrected in the revised MS.

**Modification in the MS:**

The possible primary emissions contributing to the atmospheric particles at Melpitz could come from the cities, which are tens of kilometers away from the station.

\*\*\*\*\*

Line 18: “did not increased”

**Response:**

It was corrected in the revised MS.

**Modification in the MS:**

The particle number concentration did not increase simultaneously.

Page 12, Line 10: “could result in an increasing of inorganic fraction in particle phase”

**Response:**

It was corrected in the revised MS.

**Modification in the MS:**

Both processes could result in an enhanced inorganic mass fraction in particle phase

\*\*\*\*\*

Page 13, Line 7: “While, the nitrate accounted for a minor fraction, which also observed by Zhang et al. in Pittsburgh (Zhang et al., 2004a).” (This is not even a full sentence.)

**Response:**

It was removed from the revised MS.

\*\*\*\*\*

Page 15, Line 9: Another confusing wrong use of the word “dominated”.

**Response:**

It was corrected in the revised MS.

\*\*\*\*\*

Page 17, Title: “Reference” instead of “References”

**Response:**

“Reference” was replaced by “References” in the revised manuscript.

\*\*\*\*\*

# Some insights into the condensing vapors driving new particle growth to CCN sizes on the basis of hygroscopicity measurements

Z. J. Wu<sup>1,2</sup>, L. Poulain<sup>2</sup>, W. Birmili<sup>2</sup>, J. Größ<sup>2</sup>, N. Niedermeier<sup>2</sup>, Z. B. Wang<sup>3</sup>, H. Herrmann<sup>2</sup>, A. Wiedensohler<sup>2</sup>

[1] College of Environmental Sciences and Engineering, Peking University, 100871, Beijing, China

[2] Leibniz Institute for Tropospheric Research, 04318, Leipzig, Germany

[3] Multiphase Chemistry Department, Max Planck Institute for Chemistry, Mainz 55128, Germany

Correspondence to: Zhijun Wu ([zhijunwu@pku.edu.cn](mailto:zhijunwu@pku.edu.cn))

## Abstract

New particle formation (NPF) and growth is an important source of cloud condensation nuclei (CCN). In this study, we investigated the chemical species driving new particle growth to the CCN sizes on the basis of particle hygroscopicity measurements carried out at the research station Melpitz, Germany. Three consecutive NPF events occurred during summertime were chosen as examples to perform the study. Hygroscopicity measurements showed that the (NH<sub>4</sub>)<sub>2</sub>SO<sub>4</sub>-equivalent water-soluble fraction respectively accounts for 20% and 16% of 50 and 75 nm particles during the NPF events. Numerical analysis showed the ratios of H<sub>2</sub>SO<sub>4</sub> condensational growth to the observed particle growth were 20% and 13% for 50 and 75 nm newly formed particles, respectively. Aerosol mass spectrometer measurements showed that an enhanced mass fraction of sulfate and ammonium in the newly formed particles was observed when new particle grew to the sizes larger than 30 nm shortly after the particle formation period. At a later time, the secondary organic species played a key role in the particle growth. Both hygroscopicity and AMS measurements and numerical analysis confirmed that organic compounds were major contributors driving particle growth to CCN sizes. The critical diameters at different supersaturations estimated using AMS data and  $\kappa$ -Köhler theory increased significantly during the later course of NPF events. This indicated that the enhanced organic mass fraction caused a reduction in CCN efficiency of newly formed particles. Our results implied that the CCN production associated with atmospheric nucleation may be overestimated if assuming that newly formed particles can serve as CCN in case they grow to a fixed particle size, which was used in some previous studies, especially for organic-rich environments. In our study,



the enhancement in CCN number concentration associated with individual NPF events have been 63%, 66%, and 69% for supersaturation 0.1%, 0.4%, and 0.6%, respectively.

## 1 Introduction

The formation of new particles from gaseous precursors and their subsequent growth represent a key stage in the lifecycle of atmospheric aerosol particles. This new particle formation (NPF) process represents an important source of atmospheric particles and possibly also for the number concentration of cloud condensation nuclei (CCN) (Spracklen et al., 2008; Wiedensohler et al., 2009; Wang and Penner, 2009; Laaksonen et al., 2005; Yue et al., 2011; Kazil et al., 2010; Sotiropoulou et al., 2006; Laakso et al., 2013). NPF has thus the potential to influence climatologically important processes such as precipitation patterns and Earth's energy balance (Paasonen et al., 2013). The contribution of atmospheric nucleation to the global CCN budget spans a relatively large uncertainty range, which, together with our general poor understanding of aerosol-cloud interactions, results in major uncertainties in the radiative forcing by atmospheric aerosols (Kerminen et al., 2012). Recent model studies (Spracklen et al., 2008; Merikanto et al., 2009; Westervelt et al., 2014) have attempted to elaborate on the connection between NPF and CCN production, a process that is sensitive to a number of environmental factors.

Freshly formed particles are about 1 nanometers in diameter (Kulmala et al., 2012), and they must grow tens of nanometers in order to serve as a CCN (Dusek et al., 2006; Kerminen et al., 2012). Apparently, the nucleation rate, the particle growth, and the rate by which growing particles are removed by coagulation or deposition greatly influence the CCN production associated with atmospheric nucleation (Kuang et al., 2009; Kerminen et al., 2004). From the point of view of chemical species, both sulfuric acid and organics contribute to the subsequent particle growth after nucleation (Smith et al., 2004; Pierce et al., 2011; Ehn et al., 2007; Kulmala et al., 2004; Brus et al., 2011; Kulmala et al., 2006; Sipilä et al., 2010; Zhang et al., 2004b; Kiendler-Scharr et al., 2009; Wang et al., 2010; Ristovski et al., 2010). The contribution of sulfate and organics in the particle growth seems to be strongly depending on the location (e.g. Yue et al., 2010; Boy et al., 2005). For example, sulfuric acid fully explains the particle growth observed in the polluted urban areas, Atlanta, USA (Stolzenburg et al., 2005), while it represents only 10% in Boreal forest area (Boy et al., 2005).

Due to the differences in hygroscopicity of sulfuric acid and/or its ammonium salts and secondary organic compounds (Virkkula et al., 1999; Varutbangkul et al., 2006; Tang and Munkelwitz, 1994), hygroscopicity measurements during a NPF event can provide insight into the changes in condensing vapor properties and chemical composition of newly formed particles (Hämeri et al., 2001; Ehn et al., 2007; Ristovski et al., 2010). In this study, we investigated the chemical species driving new particle growth into CCN sizes by using experimental data on particle hygroscopicity and chemical composition measured at Melpitz, Germany. In addition, the production of potential CCN associated with the NPF event was evaluated.

## 2 Measurements

Atmospheric measurements were performed at the research station Melpitz, Germany (51.54°N, 12.93°E, 86 m above sea level). The atmospheric aerosol observed at Melpitz can be regarded as representative for Central European background conditions (Birmili et al., 2009). An account of the NPF process at Melpitz and its relationship with precursor gases and meteorology can be found in Größ et al. (2015).

The data of this study were collected during the European Integrated Project on Aerosol Cloud Climate Air Quality Interactions (EUCAARI, (Kulmala et al., 2009)) intensive field campaign from May 23<sup>rd</sup> to June 8<sup>th</sup> in 2008. Table 1 summarizes the instruments and measured parameters used in this study. All instruments were set up in the same container laboratory and utilized the same air inlet. The inlet line consisted of a PM<sub>10</sub> Anderson impactor located approximately 6 m above ground level and directly followed by an automatic aerosol diffusion dryer (Tuch et al., 2009) that maintained the relative humidity in the sampling line below 30%. Particle hygroscopicity, particle number size distribution, and chemical composition of non-refractory PM<sub>1</sub> were determined using a hygroscopicity tandem differential mobility particle analyzer (H-TDMA), a Twin Differential Mobility Particle Sizer (TDMPS), and a High Resolution Time-of-flight Aerosol Mass Spectrometer (HR-ToF-AMS), respectively.

### 2.1 Particle hygroscopicity measurements

The H-TDMA used in this study has been described in previous publications in detail (Wu et al., 2011; Massling et al., 2003), and complies to the instrumental standards prescribed in Massling et al. (2011). The H-TDMA consists of three main parts: (1) A Differential Mobility Analyzer (DMA1) that selects quasi-monodisperse particles at a relative humidity below 10%, and a

Condensation Particle Counter (CPC1) that measures the particle number concentration leaving DMA1 at the selected particle size; (2) An aerosol humidifier conditioning the particles selected by DMA1 to a defined relative humidity (RH); (3) The second DMA (DMA2) coupled with another condensation particle counter (CPC2) to measure the number size distributions of the humidified aerosol. DMA2 and the aerosol humidification are placed in a temperature-controlled box. Hygroscopicity scans with 100 nm ammonium sulfate particles were performed frequently to analyze the stability of the relative humidity of 90% in the second DMA. Hygroscopicity measurements with RH between 87% and 90% were accepted for further analysis.

The hygroscopic growth factor (HGF) is defined as the ratio of the particle mobility diameter,  $D_p(RH)$ , at a given RH to the dry diameter,  $D_{p,dry}$ :

$$HGF(RH) = \frac{D_p(RH)}{D_{p,dry}} \quad [1]$$

The TDMA<sub>inv</sub> method developed by Gysel et al. (2009) was used to invert the H-TDMA data. Dry scans (RH<10%) were used to calibrate a possible offset between DMA1 and DMA2 and define the width of the H-TDMA's transfer function (Gysel et al., 2009). In this study, the particles with dry sizes of 35, 50, 75, 110, 165, and 265 nm were measured by H-TDMA at RH=90% with the time resolution of 1h. The HGFs of 35, 50, and 75 nm particles will be taken for further analysis.

The hygroscopicity parameter,  $\kappa$ , can be calculated from the HGF measured by H-TDMA (Petters and Kreidenweis, 2007):

$$\kappa_{HTDMA} = (HGF^3 - 1) \left( \frac{\exp\left(\frac{A}{D_{p,dry} \cdot HGF}\right)}{RH} - 1 \right) \quad [2]$$

$$A = \frac{4\sigma_{s/a}M_w}{RT\rho_w} \quad [3]$$

Where  $D_{p,dry}$  and HGF are the initial dry particle diameter and the hygroscopic growth factor at 90% RH measured by H-TDMA, respectively.  $\sigma_{s/a}$  is the droplet surface tension (assumed to be that of pure water,  $\sigma_{s/a}=0.0728 \text{ N m}^{-2}$ ),  $M_w$  the molecular weight of water,  $\rho_w$  the density of liquid water,  $R$  the universal gas constant, and  $T$  the absolute temperature.

## 2.2 Particle chemical composition

The Aerodyne HR-ToF-AMS (here simply referred to as AMS) (DeCarlo et al., 2006) was operated with a time resolution of 5 min. Due to the 600 °C surface temperature of the vaporizer, the AMS only analyzes the non-refractory chemical composition of the particles. Soot, crustal material, and sea-salt cannot be detected. The aerodynamic lenses have 100% transmission efficiency down to 70 nm in a vacuum aerodynamic diameter (Canagaratna et al., 2007). Therefore, based on the transmission efficiency of the aerodynamic lenses and the detected compounds, the AMS can provide the size-resolved chemical composition of sub-micrometer non-refractory aerosol particle fraction (NR-PM1) (Canagaratna et al., 2007). The vacuum aerodynamic diameter for AMS measurements was converted to mobility diameter by division of AMS vacuum aerodynamic diameter by the estimated particle density (1400 kg/m<sup>3</sup>). Hereafter, the mobility diameter is used in AMS data below. The particle density was calculated on the basis of measured chemical composition. The detail description can be found in Poulain et al. (2014).

## 2.3 Particle number size distribution

A TDMPS was deployed to measure particle number size distributions from 3-800 nm mobility diameter with a time resolution of 10 min (Birmili et al., 1999). The system consists of two Differential Mobility Analyzers (DMA, Hauke-type) and two Condensation Particle Counters (CPC, TSI model 3010 and TSI model 3025). The sheath air is circulated in closed loops for both DMAs. Evaluation of particle number size distributions includes a multiple charge inversion, the CPC efficiency and diffusional losses in the DMA and all internal and external sampling lines according to the recommendations in Wiedensohler et al. (2012).

## 3 Methodology

### 3.1 Derivation of the soluble particle fraction

Based on the Zdanovskii–Stokes–Robinson (ZSR) method (Stokes and Robinson, 1966; Zdanovskii, 1948), the HGF of a mixture can be estimated from the sum of HGF<sub>*i*</sub> of a pure component (*i*) time their respective volume fractions,  $\varepsilon_i$  (Malm and Kreidenweis, 1997):

$$\text{HGF}_{\text{mixed}} = (\sum_i \varepsilon_i \text{HGF}_i^3)^{1/3} \quad [4]$$

Here, the chemical compounds contributing to the particle growth are separated into two fractions, **i.e., soluble and insoluble fractions** (also refer to Ehn et al., 2007; Swietlicki et al., 1999). The soluble fraction is assumed as ammonium sulfate and the insoluble fraction as organic compounds. Then,  $\epsilon$  of soluble fraction can be calculated by:

$$\epsilon_{\text{soluble}} = \frac{\text{HGF}_{\text{measured}}^3 - 1}{\text{HGF}_{(\text{NH}_4)_2\text{SO}_4}^3 - 1} \quad [5]$$

where  $\text{HGF}_{\text{measured}}$  is the HGF of particle measured by H-TDMA, and  $\text{HGF}_{(\text{NH}_4)_2\text{SO}_4}$  is the HGF of pure  $(\text{NH}_4)_2\text{SO}_4$  particle with the same size. When calculating  $\text{HGF}_{(\text{NH}_4)_2\text{SO}_4}$  in different diameters, the parameterizations for  $(\text{NH}_4)_2\text{SO}_4$  water activity developed by Potukuchi and Wexler (1995) and the density reported by Tang and Munkelwitz (1994) are used. The Kelvin term was considered in the calculation.

The assumption of an insoluble organic fraction may lead to overestimate of the soluble fraction because atmospherically relevant secondary organics typically have a growth factor larger than 1 (e.g., Varutbangkul et al., 2006). This implies that in the presence of several classes of hygroscopic substances,  $\epsilon$  derived from Eq. [5] is only an “equivalent” soluble fraction (i.e. assuming ammonium sulfate as the only soluble substance).  $\epsilon_{\text{soluble}}$  is therefore an upper estimate for the true soluble volume fraction. The advantage of using the equivalent water-soluble fraction term is to be able to analyze the particle hygroscopicity independently of differences in size. The uncertainty of the estimated soluble volume fraction is around 5%, which was derived from the measurement uncertainty of HGF (2.5%) according to the error propagation function.

### 3.2 Calculation of CCN number concentration

The CCN number concentration can be estimated by integrating the particle number size distribution from the critical diameter to the maximum diameter detected by TDMPs (800 nm, above which the particle number concentration is generally negligible), assuming particles are internal mixture. The critical diameter ( $D_{\text{pcrit}}$ ) is calculated from  $\kappa$ :

$$D_{\text{Pcrit}} = \left( \frac{4A^3}{27\kappa_{\text{chem}}\ln^2 S_c} \right)^{1/3} \quad [6]$$

Here,  $D_{\text{Pcrit}}$  is the critical diameter at which 50% of the particles were activated at the supersaturation,  $S_c$  (0.1%, 0.4%, and 0.6% were chosen in this study).  $\kappa_{\text{chem}}$  is calculated from

size-resolved AMS data according to the ZSR method and  $\kappa$ -Köhler theory (Petters and Kreidenweis, 2007):

$$\kappa_{\text{chem}} = \sum_i \varepsilon_i \kappa_i \quad [7]$$

Here,  $\kappa_i$  and  $\varepsilon_i$  are the hygroscopicity parameter and volume fraction for the individual (dry) component in the mixture with  $i$ , the number of components in the mixture. The volume fraction of each chemical species in the mixture was derived from the size-resolved AMS data as described below.

Particle mass size distributions of organics, sulfate ( $\text{SO}_4^{2-}$ ), nitrate ( $\text{NO}_3^-$ ), and ammonium ( $\text{NH}_4^+$ ) ions were detected by AMS. We use a simplified ion pairing scheme as presented in Gysel et al. (2007) to convert the ion mass concentrations to the mass concentrations of their corresponding inorganic salts as listed in Table 2. The critical diameters, corresponding to supersaturation (SS) 0.2-0.6%, roughly spanned from 50 to 120 nm in mobility diameter. Therefore, by integrating the particle mass size distribution from 50 nm to 120 nm, the mass concentrations of organics,  $\text{SO}_4^{2-}$ ,  $\text{NO}_3^-$ , and  $\text{NH}_4^+$  ions was calculated to estimate  $\kappa_{\text{chem}}$ . In the same way, the chemical composition of 150-200 nm particles is used to calculate  $\kappa_{\text{chem}}$  for the critical diameter of around 170 nm, which corresponds to a supersaturation of 0.1%.

The H-TDMA-derived  $\kappa$  was not used in calculating the critical diameter. This reason is given as follows: The inconsistencies between H-TDMA-derived kappa and Cloud Condensation Nuclei Counter (CCNc)-derived  $\kappa$  have been reported in several previous studies (Good et al., 2010; Cerully et al., 2011; Irwin et al., 2010; Petters et al., 2009; Wex et al., 2009). Possible explanations are non-ideality effects in the solution droplet, surface tension reduction due to surface active substances, and the presence of slightly soluble substances which dissolve at RHs larger than the one considered in the H-TDMA (Wex et al., 2009). Due to these effects,  $\kappa$  is not necessarily constant and may vary with humidity. Extrapolating from H-TDMA data to properties at the point of activation should be done with great care (Wu et al., 2013). In addition, our previous study (Wu et al., 2013) showed that critical diameters at different supersaturations can be well-predicted using AMS data and ZSR method. Therefore, the AMS data was decided to use to estimate the critical diameters instead of H-TDMA-derived  $\kappa$ .

### 3.3 Estimation of H<sub>2</sub>SO<sub>4</sub> concentration

H<sub>2</sub>SO<sub>4</sub> concentrations were estimated using a modified version of the chemical mass balance model introduced by Weber et al. (1997), driven by solar radiation as a source of OH:

$$[\text{H}_2\text{SO}_4] = B \frac{[\cdot\text{OH}][\text{SO}_2]}{\text{CS}} \quad [\text{cm}^{-3}] \quad [8]$$

Here, [ $\cdot\text{OH}$ ] is the hydroxyl radical concentration estimated from Eq. [9] in  $\text{cm}^{-3}$ . [ $\text{SO}_2$ ] is the measured sulfur dioxide concentration in  $\text{cm}^{-3}$ .  $B$  is a constant related to the reaction rate of the two species. CS is the condensation sink (Pirjola et al., 1999) in  $\text{s}^{-1}$  calculated from the particle number size distribution adjusted to ambient relative humidity. For this adjustment, an empirical growth law based on one year of hygroscopicity measurements at Melpitz was used (Refer to Laakso et al., 2004). The term  $B[\cdot\text{OH}][\text{SO}_2]$  represents the production term of H<sub>2</sub>SO<sub>4</sub>, and CS refers to represent the loss rate of H<sub>2</sub>SO<sub>4</sub> on the pre-existing particles.  $B$  was derived by correlation analysis of measured and estimated [ $\text{H}_2\text{SO}_4$ ] for 9 days during EUCAARI-2008 during which the data capture was satisfactory. Linear regression analysis yielded a value of  $27.49 \cdot 10^{-13} \text{ cm}^3 \text{ s}^{-1}$  for  $B$ .

$$[\cdot\text{OH}] = A' \cdot \text{Rad} \quad [\text{cm}^{-3}] \quad [9]$$

where Rad is the global solar radiation flux in  $\text{W m}^{-2}$ .  $A'$  was derived by linear regression of these parameters for the EUCAARI-2008 data set, yielding a value of  $6166 \text{ m}^2 \text{ W}^{-1}$  for  $A'$ . The calculation of H<sub>2</sub>SO<sub>4</sub> concentration was done within the works of Größ et al. (2015), with details provided therein. The accuracy of simulated H<sub>2</sub>SO<sub>4</sub> concentration is estimated as follow: Percentage error =  $\text{abs}([\text{H}_2\text{SO}_4]_{\text{measured}} - [\text{H}_2\text{SO}_4]_{\text{simulated}}) * 100 / [\text{H}_2\text{SO}_4]_{\text{simulated}}$ . Here, [ $\text{H}_2\text{SO}_4$ ]<sub>measured</sub> is the sulfuric acid concentration measured during 9-day measurements for EUCAARI-2008. The percentage error is around 40%.

### 3.4 Calculation of particle formation and growth rate

Assuming a constant particle source during a time period of  $t$ , the particle formation rate ( $J_{\text{nuc}}$ ) can be expressed as (Dal Maso et al., 2005):

$$J_{\text{nuc}} = \frac{dN_{\text{nuc}}}{dt} + F_{\text{coag}} + F_{\text{growth}} \quad [10]$$

In this study,  $N_{\text{nuc}}$  is the number concentration of nucleation mode particles ranging from 3 nm to 25 nm.  $F_{\text{growth}}$  is the flux of particles out of the specified size range (3-25 nm). The newly formed

particles rarely grew beyond 25 nm before formation ended, and  $F_{\text{growth}}$  can be neglected.  $F_{\text{coag}}$  represents a loss of formed particles due to coagulation to the preexisting particle population. It can be calculated from the following equation:

$$F_{\text{coag}} = \text{CoagS}_{\text{nuc}} N_{\text{nuc}} \quad [11]$$

where  $\text{CoagS}_{\text{nuc}}$  is the coagulation sink of particles in the nucleation mode. The detailed calculation of coagulation sink is given in Deal Maso et al. (2005).

The observed particle growth rate ( $\text{GR}_{\text{obs}}$ ) can be expressed as:

$$\text{GR}_{\text{obs}} = \frac{\Delta D_m}{\Delta t} \quad [12]$$

where  $D_m$  is a geometric mean diameter of log-normal ultrafine particle mode, which has been fitted to the number size distribution (Heintzenberg, 1994).  $\text{GR}_{\text{obs}}$  means evolution of the mean diameter within a time period  $\Delta t$ .

### 3.5 Particle growth contributed by $\text{H}_2\text{SO}_4$ condensation

Theoretically, the vapor concentration required for growth rate of  $1 \text{ nm h}^{-1}$  in certain particle size ranges can be calculated according to (Nieminen et al., 2010):

$$C_{\text{GR}=1\text{nm/h}} = \frac{2\rho_v d_v}{\gamma m_v \Delta t} \cdot \sqrt{\frac{\pi m_v}{8kT}} \cdot \left[ \frac{2x_1+1}{x_1(x_1+1)} - \frac{2x_0+1}{x_0(x_0+1)} + 2\ln\left(\frac{x_1(x_0+1)}{x_0(x_1+1)}\right) \right] \quad [13]$$

here  $x_0$  and  $x_1$  are the ratios of the vapour molecule diameter ( $d_v$ ) to the initial and final particle diameter, respectively. The mass ( $m_v$ ) and density ( $\rho_v$ ) of sulfuric acid applied in this study are 135 amu and  $1650 \text{ kg/m}^3$ , respectively, corresponding to hydrated sulfuric acid molecules (Kurtén et al., 2007). It should be mentioned that equation [13] was developed specially for particles with diameter of 3-7 nm. For larger particles ( $>10 \text{ nm}$ ), this method gives similar results to that calculated using the Fuchs-Sutugin approach (Nieminen et al., 2010). The calculated  $C_{\text{GR}=1\text{nm/h}, \text{H}_2\text{SO}_4}$  may be an underestimate because it is assumed that every sulfuric acid molecule colliding with the particle is attached to it which is not necessarily the case.

Then the growth rate contributed by sulfuric acid during the time period used for the determination of GR is calculated directly as:



$$GR_{H_2SO_4} = [H_2SO_4]_{est} / C_{GR=1nm/h, H_2SO_4} \quad [14]$$

where  $[H_2SO_4]_{est}$  is the median value from the estimated sulfuric acid concentration during the timeframe for the determination of GR.

The observed growth rate can be presented as the sum of the growth rates due to  $H_2SO_4$  ( $GR_{H_2SO_4}$ ) and organic vapors ( $GR_{org}$ ) condensation (Paasonen et al., 2010):

$$GR_{obs} = GR_{H_2SO_4} + GR_{org} \quad [15]$$

By combining equations [13-15], the overall particle volume change can be separated into two fraction contributing by  $H_2SO_4$  and organic vapors condensation.

## 4 Results

### 4.1 Particle formation and growth

The previous study on the basis of long-term observations showed that the NPF events take place frequently at Melpitz, especially on April, May, and June (Hamed et al., 2010). During our field campaign (from May 23<sup>rd</sup> to June 8<sup>th</sup> in 2008), the NPF events were also observed frequently. In present study, three NPF events, which consecutively took place from June 5 to June 7, 2008, as displayed in Fig. 1 (a), are selected for further analysis. These events are the best cases which showed clear particle bursts and subsequent growth process during the entire field campaign. The starting and ending time for each event were marked in the Fig.1 (a) as NPF1, NPF2, and NPF3. The bursts in number concentration of 3-10 nm particles were observed associated with increasing ambient temperature, decreasing relative humidity (shown in Fig. 2 (b)), and increasing in estimated  $H_2SO_4$  concentration (shown in Fig. 1(b)). The CS is between 0.01 and  $0.02 \text{ s}^{-1}$  during the NPF events. As marked in Fig.1 (a), the particle number size distribution shows the new particle formed around 10:00 a.m. and then grew with time for more than 20 h. This means that the NPF is a regional event (refer to Hussein et al., 2000) and could take place over a distance of a hundred kilometers. The Fig.2 (a) displays the wind speed and wind direction during the NPF events. The wind showed a typical diurnal cycle. The wind speed was 4-5 m/s and kept a constant direction (south) during the daytime. It was static wind during nighttime. The particle formation rates ( $J_{3-25nm}$ ) were 13.5, 6.1, 9.3  $\text{cm}^{-3}\text{s}^{-1}$  on June 5, 6, and 7,

1 respectively. The highest formation rate was observed on June 5 corresponding to the highest  
2  $\text{H}_2\text{SO}_4$  concentration.

3 As indicated by the white circle in the Fig.1 (a), the  $D_m$  of log-normal ultrafine particle mode  
4 increased to around 100 nm within 24 hours. Over the time period from the beginning to the end  
5 of the NPF events as marked in Fig.1 (a), the average  $\text{GR}_{\text{obs}}$  were respectively 2.8, 3.6, and 4.4  
6  $\text{nm h}^{-1}$  for NPF events on June 5<sup>th</sup>, 6<sup>th</sup>, and 7<sup>th</sup>, 2008. One can note that the newly formed  
7 particles continued growing during the nighttime when sulfuric acid concentration was close to  
8 zero. This indicated that other species, most likely, organic compounds contributed to the particle  
9 growth during this time period.

10 There were no local emission sources in the surrounding areas of the Melpitz research station.  
11 The possible primary emissions contributing to the atmospheric particles at Melpitz could come  
12 from the cities, which are tens of kilometers away from the station. Typically, the primary  
13 particles are accompanied by trace gases, such as NO and  $\text{SO}_2$  spikes. However, such  
14 phenomena were not observed in our measurements at Melpitz. As shown in Fig.2 (c), in the  
15 early morning on 6 and 7 June, the slight enhancement of NO (a tracer for traffic related ultrafine  
16 particles (Janhäll et al., 2004)) concentration may be caused by the outflow of cities nearby  
17 Melpitz. The particle number concentration did not increase simultaneously. The ultrafine  
18 particles exhausted from car tailpipes in the cities may grow by condensation and coagulation  
19 and shift towards larger diameters and diluted by fresh air significantly with increasing distance  
20 from the roads (Zhu et al., 2002). As a result, the enhancement in ultrafine particle number  
21 concentration was not observed at the rural site of Melpitz. Therefore, the instant impacts of  
22 primary emissions on atmospheric particles were not observed during the time period focused in  
23 this study.  $\text{SO}_2$  from primary emissions could contribute to the atmospheric nucleation after  
24 being oxidized to sulfuric acid by radicals. The new particle formation associating with enhanced  
25  $\text{SO}_2$  concentration was observed by many previous studies (e.g. Birmili and Wiedensohler, 2000).  
26 Overall, the new particle formation and subsequent growth is the major source of particles, and  
27 thereby, CCN at Melpitz station.

## 28 4.2 Hygroscopicity and chemical composition of newly formed particles

29 Fig.3 displayed the size-resolved particle hygroscopicity (a),  $m/z$  44 and 57 mass concentrations  
30 (b), and mass fraction of organic, sulfate, nitrate, and ammonium in 30-100 nm (mobility

diameter) particles (c). As shown in the Fig. 3(a), peak daily  $\kappa_s$  of 50, 75, and 110 nm particles occurred afternoon and minimum appeared in the midnight. The evolution of particle hygroscopicity was very similar to those of inorganic mass fraction (sulfate+nitrate+ ammonium) in 30-100 nm particles. During the daytime,  $H_2SO_4$  concentration increased and may condense onto the particles. At the same time, the increasing ambient temperature (see Fig. 2 (b)) could drive the semi-volatile organic species in particle phase to partition to gas phase. Both processes could result in an enhanced inorganic mass fraction in particle phase, thereby enhancement in particle hygroscopicity. The decline in particle hygroscopicity took place after 15:30 (Local time) when sulfuric acid concentration decreased significantly. Simultaneously, ambient temperature decreased to an eventual nighttime minimum of around 10°C. Lower temperature facilitates the condensation of semi-volatile organic vapors onto the particles. As a result, the organic mass fraction increased significantly during the nighttime, as shown by AMS measurements (Fig.3 (c)), leading to an evident decline in particle hygroscopicity.

Table 3 summarizes the equivalent water-soluble fraction of newly formed particles when these particles grew to 35, 50, and 75 nm, respectively. Here, the equivalent water-soluble fraction is corresponding to the H-TDMA measurement points at which the  $D_m$  of ultrafine particle mode reached 35, 50, and 75 nm. On June 7, the equivalent water-soluble fraction of 35 nm newly formed particles was 34%. It decreased to 23% when particle grew to 50 nm, further, reduced to 17% when particles reached to 75 nm. On June 5 and 6, the hygroscopicity of newly formed particles decreased with increasing particle size, as well. It implies that a large fraction of species contributing to particle growth was organics, which are typically less water soluble. This can be confirmed by AMS measurements showing that organic fraction in particles increased at a relatively later time of the NPF event (see Fig. 3(c)). The contribution of  $H_2SO_4$  condensation to particle growth was estimated using the method introduced in section 3.5 for different particle sizes. The ratios of  $H_2SO_4$  condensational growth to the observed particle growth ( $F_{GR-H_2SO_4} = GR_{H_2SO_4} / GR_{obs}$ ) are given in the table 3. For example, on June 7,  $F_{GR-H_2SO_4}$  was 30% for 35 nm particles, meaning that  $H_2SO_4$  condensation only contributed 30% of the observed particle growth. With increasing particle size, the contribution of  $H_2SO_4$  condensation decreased, as shown in Table 3. This was consistent with the changes in the equivalent water-soluble fraction of newly formed particles. Both particle hygroscopicity measurements and numerical analysis showed that organics were potentially major contributors to the particle growth.

As displayed in Fig.3 (c), the organic compounds were dominating species in 30-100 nm particles in the particle formation period (indicated by grey dashed line). In this period, most of newly formed particles were smaller than 30 nm, as shown in Fig. 1 (a). They are too small to be detected by HR-ToF-AMS. Therefore, AMS measurements cannot provide proper information on chemical composition of newly formed particles in particle formation period. After around 12:00, the newly formed particles grew beyond 30 nm. Simultaneously, an obvious increase in sulfate and ammonium mass fraction in 30-100 nm particles was observed. This indicates that the newly formed particles were dominated by sulfate and ammonium. After 3:00 p.m., the organic mass fraction increased and reached its maximum at midnight on each day, indicating that organics played a key role in the particle growth at a later time of the NPF event. The mass fraction of ion fragments  $m/z$  44 and 57 in 30-100 nm particles are shown in the Fig. 3(b). The  $m/z$  44 ( $\text{CO}_2^+$  ion fragment) is a tracer for secondary organic aerosol, while  $m/z$  57 ( $\text{C}_4\text{H}_9^+$ ) is generally associated with primary organics from combustion sources (Zhang et al., 2004a). The  $m/z$  57 mass concentration was close to zero during the events. Compared  $m/z$  57, the  $m/z$  44 mass concentration were considerable, indicating that the organics contributing to particle growth was mainly secondary organic species.

#### 4.3 Enhancement in CCN number concentration during the NPF events

The critical diameters and CCN number concentrations at different supersaturations during the NPF events are displayed in the Fig. 4. The critical diameters at different supersaturations decreased during the first several hours of the NPF events and enhanced at a later time of the NPF event. This was consistent with the variations in particle hygroscopic growth at  $\text{RH}=90\%$  above-mentioned (see Fig. 3(a)). As shown in the Fig. 4(b), the CCN number concentration clearly increased significantly during the NPF events. The minimum in CCN number concentration was observed during the period of particle formation and the maximum appeared at the end of the NPF events.

The NPF events occurred on June 5, 6, and 7 were typical regional cases. The enhancement in CCN number concentration caused by atmospheric nucleation was evaluated by comparing the average CCN number concentrations over two hours prior to the beginning of the event (the period  $t_1$  marked in Fig. 4) with the same time period before the end of the events (the period  $t_2$  marked in Fig. 4). The ratios of average CCN number concentration over  $t_2$  to  $t_1$  were

1 respectively 1.9, 2.0, and 1.5 for 0.1%, 0.4%, and 0.6% SS. On average, the enhancement ratios  
2 in CCN number concentration associated with individual NPF events were 63%, 66%, and 69%  
3 for 0.1, 0.4, and 0.6% SS, respectively. The absolute increases in CCN number concentrations  
4 associated with each event were 162, 931, and 756  $\text{\#}/\text{cm}^3$ , on average.

5 Atmospheric boundary layer development and turbulent mixing will impact on NPF (Boy et al.,  
6 2006; Boy et al., 2003; Altstädter et al., 2015), and consequently on its CCN products. It is hard  
7 task to quantify the changes in CCN number due to boundary layer dynamics. In this study, the  
8 enhancement in CCN number concentration caused by atmospheric nucleation was evaluated by  
9 a ratio of CCN number during the same period on different days, and not an absolute value. Here  
10 we assume that the weather condition and boundary layer height were similar during two time  
11 periods (see meteorological parameters in Fig. 3). Therefore, we assumed that the effect of  
12 boundary layer dynamics on the change in CCN number concentration could be ignored.

13 Several previous studies reported that the enhancement in CCN number concentration associated  
14 with atmospheric nucleation varied significantly in different environments. At the Finnish sub-  
15 Arctic Pallas station, a  $210 \pm 110\%$  increase in the number concentration of 80 nm particles was  
16 observed from the beginning of a nucleation event to the end of the event (Asmi et al., 2011). At  
17 a forested site (SMEAR II station in Hyytiälä) in Southern Finland, nucleation enhanced CCN  
18 number concentration by 70 to 110%, varying with the supersaturation level (Sihto et al., 2011).  
19 In a polluted urban area, Beijing, China, the average CCN enhancement factors were between  
20 about 1.5 and 2.5 (Yue et al., 2011; Wiedensohler et al., 2009). In Boulder, CO, Atlanta, GA, and  
21 Tecamac, Mexico, the pre-existing CCN number concentration increased on average by a factor  
22 of 3.8 as a result of new particle formation (Kuang et al., 2009). Overall, the enhancement in  
23 CCN number concentration associated with atmospheric nucleation varied significantly in  
24 different environments. Please note that the methods for defining the enhancement factors used  
25 in the existing literature were very different. Therefore, a general conclusion on how significant  
26 NPF and growth process contributes to CCN budget cannot be drawn, currently.

## 27 **5 Discussion**

28 The above field observations clearly showed that newly formed particles had the ability to grow  
29 into CCN sizes within several hours at Melpitz. The particle hygroscopicity measurements  
30 strongly suggested that organic compounds were the major contributors driving particle growth

into CCN sizes. The previous studies performed in clean atmosphere also showed that the newly formed particles mainly consist of organics. For examples, sulfuric acid is able to account for roughly 30% of the growth rate of newly formed particles in the rural atmosphere of Hohenpeissenberg, Southern Germany (Birmili et al., 2003), and only around 10% in the boreal forest area of Finland (Boy et al., 2005). However, In the polluted atmosphere of Atlanta, USA, the available amount of sulfuric acid was sufficient to explain all of the observed particle growth (Stolzenburg et al., 2005). At Melpitz, biogenic volatile organic compounds (BVOCs) emitted from biological activities are dominating volatile organic compounds (Mutzel et al., 2015) and lead to an organic-rich environment during the summertime. The oxidation products of BVOCs may be responsible for the new particle growth.

We note that the condensation of organics lead to a rapid particle growth when sulfuric acid concentration was close to zero during the nighttime, as shown in Fig. 1. The organic condensing materials with low hygroscopicity reduced CCN efficiency of the new particles, as indicated by critical diameters given in Fig. 4. Such phenomenon was also reported by Dusek et al. (2010). They showed that enhanced organic mass fraction caused a reduction in CCN efficiency of small particles during the new particle formation. These results implied that the CCN production associated with atmospheric nucleation may be overestimated if assuming that new particles can serve as CCN in case they grow to a fixed particle size (Such as Asmi et al., 2011), especially for organic-rich environments. In our case, the mean critical diameter is around 50 nm at SS=0.6%. Assuming a constant critical diameter of 50 nm at SS=0.6%, the CCN number concentration was averagely 1.13 times of that with varied critical diameters during the NPF events. Under similar conditions, the CCN number concentration at SS=0.4% with a constant critical diameter of 70 nm was 1.15 times of that with varied critical diameters.

## 6 Conclusions

In this study, the particle number size distribution, particle hygroscopicity, and particle chemical composition during three regional NPF events were measured to investigate the new particle growth process and its effects on CCN activity. The particle formation rates ( $J_{3-25\text{nm}}$ ) were 13.5, 6.1, 9.3  $\text{cm}^{-3}\text{s}^{-1}$ , and the particle growth rates were 2.8, 3.6, and 4.4 nm/h for NPF events on June 5, 6 and 7, 2008, respectively.

1 The (NH<sub>4</sub>)<sub>2</sub>SO<sub>4</sub>-equivalent water-soluble fraction accounted for 20% and 16% of 50 and 75 nm  
2 newly formed particles, respectively. AMS measurements showed that the sulfate and  
3 ammonium were dominating chemical species when newly formed particles grew beyond 30 nm  
4 shortly after particle formation period. At a later time of NPF event, the organics played a key  
5 role in the particle growth. The analysis on the fragment m/z 44 and 57 showed that the organics  
6 contributing to particle growth was mainly secondary organic species. The particle  
7 hygroscopicity and chemical composition measurements and numerical calculation confirmed  
8 that organic compounds were major contributors driving particles growth to CCN sizes.

9 The step-wised increase in CCN number concentration during three consecutive NPF events was  
10 observed. On average, the enhancement ratios in CCN number concentration associated with  
11 individual NPF events are 63%, 66%, 69% for 0.1, 0.4, and 0.6% SS, respectively. We found  
12 that the new particles hygroscopicity decreased significantly with condensational growth of  
13 organic compounds, which are generally less water soluble. Correspondingly, the critical  
14 diameters at a certain supersaturation increased, indicating that enhanced organic mass fraction  
15 caused a reduction in CCN efficiency of newly formed particles during the new particle  
16 formation. Our results implied that the CCN production associated with atmospheric nucleation  
17 may be overestimated if assuming that new particles can serve as CCN in case they grow to a  
18 fixed particle size, which was used in some previous studies, especially for organic-rich  
19 environments.

## 20 Acknowledgements

21 The data analysis work done by the first author is supported by National Natural Science  
22 Foundation of China (41475127). Data collection was supported by the European Commission  
23 projects EUSAAR (European Supersites for Atmospheric Aerosol Research), EUCAARI  
24 (European Integrated project on Aerosol Cloud Climate and Air Quality Interactions) FP6-  
25 036833-2-EUCAARI, and the German Federal Environment Ministry (BMU) grant F&E  
26 370343200. We acknowledge Friederike Kinder, Andreas Maßling, and Thomas Tuch for their  
27 contributions related to H-TDMA and TDMPS data acquisition.



## References

- Altstädter, B., Platis, A., Wehner, B., Scholtz, A., Wildmann, N., Hermann, M., Käthner, R., Baars, H., Bange, J., and Lampert, A.: ALADINA – an unmanned research aircraft for observing vertical and horizontal distributions of ultrafine particles within the atmospheric boundary layer, *Atmos. Meas. Tech.*, 8, 1627-1639, 10.5194/amt-8-1627-2015, 2015.
- Asmi, E., Kivekäs, N., Kerminen, V. M., Komppula, M., Hyvärinen, A. P., Hatakka, J., Viisanen, Y., and Lihavainen, H.: Secondary new particle formation in Northern Finland Pallas site between the years 2000 and 2010, *Atmos. Chem. Phys.*, 11, 12959-12972, 10.5194/acp-11-12959-2011, 2011.
- Birmili, W., Stratmann, F., and Wiedensohler, A.: Design of a DMA-based size spectrometer for a large particle size range and stable operation, *J. Aerosol Sci.*, 30, 549-553, 1999.
- Birmili, W., and Wiedensohler, A.: New particle formation in the continental boundary layer: Meteorological and gas phase parameter influence, *Geophysical Research Letters*, 27, 3325-3328, 10.1029/1999GL011221, 2000.
- Birmili, W., Berresheim, H., Plass-Dülmer, C., Elste, T., Gilge, S., Wiedensohler, A., and Uhrner, U.: The Hohenpeissenberg aerosol formation experiment (HAFEX): a long-term study including size-resolved aerosol, H<sub>2</sub>SO<sub>4</sub>, OH, and monoterpenes measurements, *Atmos. Chem. Phys.*, 3, 361-376, 10.5194/acp-3-361-2003, 2003.
- Birmili, W., Weinhold, K., Nordmann, S., Wiedensohler, A., Spindler, G., Müller, K., Herrmann, H., Gnauk, T., Pitz, M., Cyrys, J., Flentje, H., Nickel, C., Kuhlbusch, T. A. J., and Löschau, G.: Atmospheric aerosol measurements in the German Ultrafine Aerosol Network (GUAN): Part 1 - soot and particle number size distribution, *Gefährst. Reinh. Luft.*, 69, 137-145, 2009.
- Boy, M., Rannik, Ü., Lehtinen, K. E. J., Tarvainen, V., Hakola, H., and Kulmala, M.: Nucleation events in the continental boundary layer: Long-term statistical analyses of aerosol relevant characteristics, *Journal of Geophysical Research: Atmospheres*, 108, n/a-n/a, 10.1029/2003JD003838, 2003.
- Boy, M., Kulmala, M., Ruuskanen, T. M., Pihlatie, M., Reissell, A., Aalto, P. P., Keronen, P., Dal Maso, M., Hellen, H., Hakola, H., Jansson, R., Hanke, M., and Arnold, F.: Sulphuric acid closure and contribution to nucleation mode particle growth, *Atmos. Chem. Phys.*, 5, 863-878, 10.5194/acp-5-863-2005, 2005.
- Boy, M., Hellmuth, O., Korhonen, H., Nilsson, E. D., ReVelle, D., Turnipseed, A., Arnold, F., and Kulmala, M.: MALTE – model to predict new aerosol formation in the lower troposphere, *Atmos. Chem. Phys.*, 6, 4499-4517, 10.5194/acp-6-4499-2006, 2006.



- 1 Brus, D., Neitola, K., Hyvärinen, A. P., Petäjä, T., Vanhanen, J., Sipilä, M., Paasonen, P., Kulmala, M.,  
2 and Lihavainen, H.: Homogenous nucleation of sulfuric acid and water at close to atmospherically  
3 relevant conditions, *Atmos. Chem. Phys.*, 11, 5277-5287, 10.5194/acp-11-5277-2011, 2011.
- 4 Canagaratna, M. R., Jayne, J. T., Jimenez, J. L., Allan, J. D., Alfarra, M. R., Zhang, Q., Onasch, T. B.,  
5 Drewnick, F., Coe, H., Middlebrook, A., Delia, A., Williams, L. R., Trimborn, A. M., Northway, M. J.,  
6 DeCarlo, P. F., Kolb, C. E., Davidovits, P., and Worsnop, D. R.: Chemical and microphysical  
7 characterization of ambient aerosols with the aerodyne aerosol mass spectrometer, *Mass Spectrometry*  
8 *Reviews*, 26, 185-222, 10.1002/mas.20115, 2007.
- 9 Cerully, K. M., Raatikainen, T., Lance, S., Tkacik, D., Tiitta, P., Petäjä, T., Ehn, M., Kulmala, M.,  
10 Worsnop, D. R., Laaksonen, A., Smith, J. N., and Nenes, A.: Aerosol hygroscopicity and CCN activation  
11 kinetics in a boreal forest environment during the 2007 EUCAARI campaign, *Atmos. Chem. Phys.*, 11,  
12 12369-12386, 10.5194/acp-11-12369-2011, 2011.
- 13 Dal Maso, M., Kulmala, M., Riipinen, I., Wagner, R., Hussein, T., Aalto, P. P., and Lehtinen, K. E.:  
14 Formation and growth of fresh atmospheric aerosols: eight years of aerosol size distribution data from  
15 SMEAR II, Hyytiälä, Finland, *Boreal Environment Research*, 10, 323, 2005.
- 16 DeCarlo, P. F., Kimmel, J. R., Trimborn, A., Northway, M. J., Jayne, J. T., Aiken, A. C., Gonin, M.,  
17 Fuhrer, K., Horvath, T., Docherty, K. S., Worsnop, D. R., and Jimenez, J. L.: Field-Deployable, High-  
18 Resolution, Time-of-Flight Aerosol Mass Spectrometer, *Analytical Chemistry*, 78, 8281-8289,  
19 10.1021/ac061249n, 2006.
- 20 Dusek, U., Frank, G. P., Hildebrandt, L., Curtius, J., Schneider, J., Walter, S., Chand, D., Drewnick, F.,  
21 Hings, S., Jung, D., Borrmann, S., and Andreae, M. O.: Size Matters More Than Chemistry for Cloud-  
22 Nucleating Ability of Aerosol Particles, *Science*, 312, 1375-1378, 10.1126/science.1125261, 2006.
- 23 Dusek, U., Frank, G. P., Curtius, J., Drewnick, F., Schneider, J., Kürten, A., Rose, D., Andreae, M. O.,  
24 Borrmann, S., and Pöschl, U.: Enhanced organic mass fraction and decreased hygroscopicity of cloud  
25 condensation nuclei (CCN) during new particle formation events, *Geophysical Research Letters*, 37, n/a-  
26 n/a, 10.1029/2009GL040930, 2010.
- 27 Ehn, M., Petäjä, T., Aufmhoff, H., Aalto, P., Hämeri, K., Arnold, F., Laaksonen, A., and Kulmala, M.:  
28 Hygroscopic properties of ultrafine aerosol particles in the boreal forest: diurnal variation, solubility and  
29 the influence of sulfuric acid, *Atmos. Chem. Phys.*, 7, 211-222, 10.5194/acp-7-211-2007, 2007.
- 30 Good, N., Topping, D. O., Allan, J. D., Flynn, M., Fuentes, E., Irwin, M., Williams, P. I., Coe, H., and  
31 McFiggans, G.: Consistency between parameterisations of aerosol hygroscopicity and CCN activity  
32 during the RHAMBLE discovery cruise, *Atmos. Chem. Phys.*, 10, 3189-3203, 10.5194/acp-10-3189-2010,  
33 2010.
- 34 Größ, J., Birmili, W., Hamed, A., Sonntag, A., Wiedensohler, A., Spindler, G., Maninnen, H. E.,  
35 Nieminen, T., Kulmala, M., Hörrak, U., and Plass-Dülmer, C.: Evolution of gaseous precursors and  
36 meteorological parameters during new particle formation events in the Central European boundary layer,  
37 *Atmos. Chem. Phys. Discuss.*, 15, 2305-2353, 10.5194/acpd-15-2305-2015, 2015.

- 1 Gysel, M., Crosier, J., Topping, D. O., Whitehead, J. D., Bower, K. N., Cubison, M. J., Williams, P. I.,  
2 Flynn, M. J., McFiggans, G. B., and Coe, H.: Closure study between chemical composition and  
3 hygroscopic growth of aerosol particles during TORCH2, *Atmos. Chem. Phys.*, 7, 6131-6144,  
4 10.5194/acp-7-6131-2007, 2007.
- 5 Gysel, M., McFiggans, G. B., and Coe, H.: Inversion of tandem differential mobility analyser (TDMA)  
6 measurements, *Journal of Aerosol Science*, 40, 134-151, 10.1016/j.jaerosci.2008.07.013, 2009.
- 7 Hämeri, K., Väkevä, M., Aalto, P. P., Kulmala, M., Swietlicki, E., Zhou, J., Seidl, W., Becker, E., and  
8 O'Dowd, C. D.: Hygroscopic and CCN properties of aerosol particles in boreal forests, *Tellus B*, 53, 359-  
9 379, 10.1034/j.1600-0889.2001.530404.x, 2001.
- 10 Hamed, A., Birmili, W., Joutsensaari, J., Mikkonen, S., Asmi, A., Wehner, B., Spindler, G., Jaatinen, A.,  
11 Wiedensohler, A., Korhonen, H., Lehtinen, K. E. J., and Laaksonen, A.: Changes in the production rate of  
12 secondary aerosol particles in Central Europe in view of decreasing SO<sub>2</sub> emissions between 1996 and  
13 2006, *Atmos. Chem. Phys.*, 10, 1071-1091, 10.5194/acp-10-1071-2010, 2010.
- 14 Heintzenberg, J.: Properties of the Log-Normal Particle Size Distribution, *Aerosol Science and*  
15 *Technology*, 21, 46-48, 10.1080/02786829408959695, 1994.
- 16 Hussein, T., Aalto, P. P., and Lehtinen, K. E. J.: Formation and growth of fresh atmospheric aerosols:  
17 eight years of aerosol size distribution data from SMEAR II, Hyytiälä, Finland, 2000.
- 18 Irwin, M., Good, N., Crosier, J., Choularton, T. W., and McFiggans, G.: Reconciliation of measurements  
19 of hygroscopic growth and critical supersaturation of aerosol particles in central Germany, *Atmos. Chem.*  
20 *Phys.*, 10, 11737-11752, 10.5194/acp-10-11737-2010, 2010.
- 21 Janhäll, S., M. Jonsson, Å., Molnár, P., A. Svensson, E., and Hallquist, M.: Size resolved traffic emission  
22 factors of submicrometer particles, *Atmospheric Environment*, 38, 4331-4340,  
23 <http://dx.doi.org/10.1016/j.atmosenv.2004.04.018>, 2004.
- 24 Kazil, J., Stier, P., Zhang, K., Quaas, J., Kinne, S., O'Donnell, D., Rast, S., Esch, M., Ferrachat, S.,  
25 Lohmann, U., and Feichter, J.: Aerosol nucleation and its role for clouds and Earth's radiative forcing in  
26 the aerosol-climate model ECHAM5-HAM, *Atmos. Chem. Phys.*, 10, 10733-10752, 10.5194/acp-10-  
27 10733-2010, 2010.
- 28 Kerminen, V.-M., Lehtinen, K. E. J., Anttila, T., and Kulmala, M.: Dynamics of atmospheric nucleation  
29 mode particles: a timescale analysis, *Tellus B*, 56, 135-146, 10.3402/tellusb.v56i2.16411, 2004.
- 30 Kerminen, V. M., Paramonov, M., Anttila, T., Riipinen, I., Fountoukis, C., Korhonen, H., Asmi, E.,  
31 Laakso, L., Lihavainen, H., Swietlicki, E., Svenningsson, B., Asmi, A., Pandis, S. N., Kulmala, M., and  
32 Petäjä, T.: Cloud condensation nuclei production associated with atmospheric nucleation: a synthesis  
33 based on existing literature and new results, *Atmos. Chem. Phys.*, 12, 12037-12059, 10.5194/acp-12-  
34 12037-2012, 2012.

- 1 Kiendler-Scharr, A., Wildt, J., Maso, M. D., Hohaus, T., Kleist, E., Mentel, T. F., Tillmann, R., Uerlings,  
2 R., Schurr, U., and Wahner, A.: New particle formation in forests inhibited by isoprene emissions, *Nature*,  
3 461, 381-384, [http://www.nature.com/nature/journal/v461/n7262/supinfo/nature08292\\_S1.html](http://www.nature.com/nature/journal/v461/n7262/supinfo/nature08292_S1.html), 2009.
- 4 Kuang, C., McMurry, P. H., and McCormick, A. V.: Determination of cloud condensation nuclei  
5 production from measured new particle formation events, *Geophysical Research Letters*, 36, L09822,  
6 10.1029/2009GL037584, 2009.
- 7 Kulmala, M., Laakso, L., Lehtinen, K. E. J., Riipinen, I., Dal Maso, M., Anttila, T., Kerminen, V. M.,  
8 Hörrak, U., Vana, M., and Tammet, H.: Initial steps of aerosol growth, *Atmos. Chem. Phys.*, 4, 2553-  
9 2560, 10.5194/acp-4-2553-2004, 2004.
- 10 Kulmala, M., Lehtinen, K. E. J., and Laaksonen, A.: Cluster activation theory as an explanation of the  
11 linear dependence between formation rate of 3nm particles and sulphuric acid concentration, *Atmos.*  
12 *Chem. Phys.*, 6, 787-793, 10.5194/acp-6-787-2006, 2006.
- 13 Kulmala, M., Asmi, A., Lappalainen, H. K., Carslaw, K. S., Pöschl, U., Baltensperger, U., Hov, Ø.,  
14 Brenquier, J. L., Pandis, S. N., Facchini, M. C., Hansson, H. C., Wiedensohler, A., and O'Dowd, C. D.:  
15 Introduction: European Integrated Project on Aerosol Cloud Climate and Air Quality interactions  
16 (EUCAARI) – integrating aerosol research from nano to global scales, *Atmos. Chem. Phys.*, 9, 2825-  
17 2841, 10.5194/acp-9-2825-2009, 2009.
- 18 Kulmala, M., Petäjä, T., Nieminen, T., Sipilä, M., Manninen, H. E., Lehtipalo, K., Dal Maso, M., Aalto, P.  
19 P., Junninen, H., Paasonen, P., Riipinen, I., Lehtinen, K. E. J., Laaksonen, A., and Kerminen, V.-M.:  
20 Measurement of the nucleation of atmospheric aerosol particles, *Nat. Protocols*, 7, 1651-1667,  
21 <http://www.nature.com/nprot/journal/v7/n9/abs/nprot.2012.091.html#supplementary-information>, 2012.
- 22 Kurtén, T., Torpo, L., Ding, C.-G., Vehkamäki, H., Sundberg, M. R., Laasonen, K., and Kulmala, M.: A  
23 density functional study on water-sulfuric acid-ammonia clusters and implications for atmospheric cluster  
24 formation, *Journal of Geophysical Research: Atmospheres*, 112, n/a-n/a, 10.1029/2006jd007391, 2007.
- 25 Laakso, L., Petäjä, T., Lehtinen, K. E. J., Kulmala, M., Paatero, J., Hörrak, U., Tammet, H., and  
26 Joutsensaari, J.: Ion production rate in a boreal forest based on ion, particle and radiation measurements,  
27 *Atmos. Chem. Phys.*, 4, 1933-1943, 10.5194/acp-4-1933-2004, 2004.
- 28 Laakso, L., Merikanto, J., Vakkari, V., Laakso, H., Kulmala, M., Molefe, M., Kgabi, N., Mabaso, D.,  
29 Carslaw, K. S., Spracklen, D. V., Lee, L. A., Reddington, C. L., and Kerminen, V. M.: Boundary layer  
30 nucleation as a source of new CCN in savannah environment, *Atmos. Chem. Phys.*, 13, 1957-1972,  
31 10.5194/acp-13-1957-2013, 2013.
- 32 Laaksonen, A., Hamed, A., Joutsensaari, J., Hiltunen, L., Cavalli, F., Junkermann, W., Asmi, A., Fuzzi, S.,  
33 and Facchini, M. C.: Cloud condensation nucleus production from nucleation events at a highly polluted  
34 region, *Geophys. Res. Lett.*, 32, L06812, 10.1029/2004gl022092, 2005.

- 1 Malm, W. C., and Kreidenweis, S. M.: The effects of models of aerosol hygroscopicity on the  
2 apportionment of extinction, *Atmospheric Environment*, 31, 1965-1976, 10.1016/s1352-2310(96)00355-x,  
3 1997.
- 4 Massling, A., Wiedensohler, A., Busch, B., Neusüß, C., Quinn, P., Bates, T., and Covert, D.: Hygroscopic  
5 properties of different aerosol types over the Atlantic and Indian Oceans, *Atmos. Chem. Phys.*, 3, 1377-  
6 1397, 10.5194/acp-3-1377-2003, 2003.
- 7 Massling, A., Niedermeier, N., Hennig, T., Fors, E. O., Swietlicki, E., Ehn, M., Hämeri, K., Villani, P.,  
8 Laj, P., Good, N., McFiggans, G., and Wiedensohler, A.: Results and recommendations from an  
9 intercomparison of six Hygroscopicity-TDMA systems, *Atmos. Meas. Tech.*, 4, 485-497, 10.5194/amt-4-  
10 485-2011, 2011.
- 11 Merikanto, J., Spracklen, D. V., Mann, G. W., Pickering, S. J., and Carslaw, K. S.: Impact of nucleation  
12 on global CCN, *Atmos. Chem. Phys.*, 9, 8601-8616, 10.5194/acp-9-8601-2009, 2009.
- 13 Mutzel, A., Poulain, L., Berndt, T., Iinuma, Y., Rodigast, M., Böge, O., Richters, S., Spindler, G., Sipilä,  
14 M., Jokinen, T., Kulmala, M., and Herrmann, H.: Highly Oxidized Multifunctional Organic Compounds  
15 Observed in Tropospheric Particles: A Field and Laboratory Study, *Environmental Science & Technology*,  
16 49, 7754-7761, 10.1021/acs.est.5b00885, 2015.
- 17 Nieminen, T., Lehtinen, K. E. J., and Kulmala, M.: Sub-10 nm particle growth by vapor condensation –  
18 effects of vapor molecule size and particle thermal speed, *Atmos. Chem. Phys.*, 10, 9773-9779,  
19 10.5194/acp-10-9773-2010, 2010.
- 20 Paasonen, P., Nieminen, T., Asmi, E., Manninen, H. E., Petäjä, T., Plass-Dülmer, C., Flentje, H., Birmili,  
21 W., Wiedensohler, A., Hörrak, U., Metzger, A., Hamed, A., Laaksonen, A., Facchini, M. C., Kerminen, V.  
22 M., and Kulmala, M.: On the roles of sulphuric acid and low-volatility organic vapours in the initial steps  
23 of atmospheric new particle formation, *Atmos. Chem. Phys.*, 10, 11223-11242, 10.5194/acp-10-11223-  
24 2010, 2010.
- 25 Paasonen, P., Asmi, A., Petaja, T., Kajos, M. K., Aijala, M., Junninen, H., Holst, T., Abbatt, J. P. D.,  
26 Arneth, A., Birmili, W., van der Gon, H. D., Hamed, A., Hoffer, A., Laakso, L., Laaksonen, A., Richard  
27 Leaitch, W., Plass-Dulmer, C., Pryor, S. C., Raisanen, P., Swietlicki, E., Wiedensohler, A., Worsnop, D.  
28 R., Kerminen, V.-M., and Kulmala, M.: Warming-induced increase in aerosol number concentration  
29 likely to moderate climate change, *Nature Geosci*, 6, 438-442, 10.1038/ngeo1800  
30 <http://www.nature.com/ngeo/journal/v6/n6/abs/ngeo1800.html#supplementary-information>, 2013.
- 31 Petters, M. D., and Kreidenweis, S. M.: A single parameter representation of hygroscopic growth and  
32 cloud condensation nucleus activity, *Atmos. Chem. Phys.*, 7, 1961-1971, 10.5194/acp-7-1961-2007, 2007.
- 33 Petters, M. D., Wex, H., Carrico, C. M., Hallbauer, E., Massling, A., McMeeking, G. R., Poulain, L., Wu,  
34 Z., Kreidenweis, S. M., and Stratmann, F.: Towards closing the gap between hygroscopic growth and  
35 activation for secondary organic aerosol – Part 2: Theoretical approaches, *Atmos. Chem. Phys.*, 9, 3999-  
36 4009, 10.5194/acp-9-3999-2009, 2009.

- 1 Pierce, J. R., Riipinen, I., Kulmala, M., Ehn, M., Petäjä, T., Junninen, H., Worsnop, D. R., and Donahue,  
2 N. M.: Quantification of the volatility of secondary organic compounds in ultrafine particles during  
3 nucleation events, *Atmos. Chem. Phys.*, 11, 9019-9036, 10.5194/acp-11-9019-2011, 2011.
- 4 Pirjola, L., Kulmala, M., Wilck, M., Bischoff, A., Stratmann, F., and Otto, E.: FORMATION OF  
5 SULPHURIC ACID AEROSOLS AND CLOUD CONDENSATION NUCLEI: AN EXPRESSION FOR  
6 SIGNIFICANT NUCLEATION AND MODEL COMPARISON, *Journal of Aerosol Science*, 30, 1079-  
7 1094, [http://dx.doi.org/10.1016/S0021-8502\(98\)00776-9](http://dx.doi.org/10.1016/S0021-8502(98)00776-9), 1999.
- 8 Potukuchi, S., and Wexler, A. S.: Identifying solid-aqueous phase transitions in atmospheric aerosols—I.  
9 Neutral-acidity solutions, *Atmospheric Environment*, 29, 1663-1676, [http://dx.doi.org/10.1016/1352-](http://dx.doi.org/10.1016/1352-2310(95)00074-9)  
10 [2310\(95\)00074-9](http://dx.doi.org/10.1016/1352-2310(95)00074-9), 1995.
- 11 Poulain, L., Birmili, W., Canonaco, F., Crippa, M., Wu, Z. J., Nordmann, S., Spindler, G., Prévôt, A. S.  
12 H., Wiedensohler, A., and Herrmann, H.: Chemical mass balance of 300 °C non-volatile particles at the  
13 tropospheric research site Melpitz, Germany, *Atmos. Chem. Phys.*, 14, 10145-10162, 10.5194/acp-14-  
14 10145-2014, 2014.
- 15 Ristovski, Z. D., Suni, T., Kulmala, M., Boy, M., Meyer, N. K., Duplissy, J., Turnipseed, A., Morawska,  
16 L., and Baltensperger, U.: The role of sulphates and organic vapours in growth of newly formed particles  
17 in a eucalypt forest, *Atmos. Chem. Phys.*, 10, 2919-2926, 10.5194/acp-10-2919-2010, 2010.
- 18 Sihto, S. L., Mikkilä, J., Vanhanen, J., Ehn, M., Liao, L., Lehtipalo, K., Aalto, P. P., Duplissy, J., Petäjä,  
19 T., Kerminen, V. M., Boy, M., and Kulmala, M.: Seasonal variation of CCN concentrations and aerosol  
20 activation properties in boreal forest, *Atmos. Chem. Phys.*, 11, 13269-13285, 10.5194/acp-11-13269-2011,  
21 2011.
- 22 Sipilä, M., Berndt, T., Petäjä, T., Brus, D., Vanhanen, J., Stratmann, F., Patokoski, J., Mauldin, R. L.,  
23 Hyvärinen, A.-P., Lihavainen, H., and Kulmala, M.: The Role of Sulfuric Acid in Atmospheric  
24 Nucleation, *Science*, 327, 1243-1246, 2010.
- 25 Smith, J. N., Moore, K. F., McMurry, P. H., and Eisele, F. L.: Atmospheric Measurements of Sub-20 nm  
26 Diameter Particle Chemical Composition by Thermal Desorption Chemical Ionization Mass Spectrometry,  
27 *Aerosol Science and Technology*, 38, 100-110, 10.1080/02786820490249036, 2004.
- 28 Sotiropoulou, R. E. P., Tagaris, E., Pilinis, C., Anttila, T., and Kulmala, M.: Modeling New Particle  
29 Formation During Air Pollution Episodes: Impacts on Aerosol and Cloud Condensation Nuclei, *Aerosol*  
30 *Science and Technology*, 40, 557-572, 10.1080/02786820600714346, 2006.
- 31 Spracklen, D. V., Carslaw, K. S., Kulmala, M., Kerminen, V.-M., Sihto, S.-L., Riipinen, I., Merikanto, J.,  
32 Mann, G. W., Chipperfield, M. P., Wiedensohler, A., Birmili, W., and Lihavainen, H.: Contribution of  
33 particle formation to global cloud condensation nuclei concentrations, *Geophys. Res. Lett.*, 35, L06808,  
34 10.1029/2007gl033038, 2008.
- 35 Stokes, R. H., and Robinson, R. A.: Interactions in Aqueous Nonelectrolyte Solutions. I. Solute-Solvent  
36 Equilibria, *Journal of Physical Chemistry*, 70, 2126-2130, 1966.

- 1 Stolzenburg, M. R., McMurry, P. H., Sakurai, H., Smith, J. N., Mauldin, R. L., Eisele, F. L., and Clement,  
2 C. F.: Growth rates of freshly nucleated atmospheric particles in Atlanta, *Journal of Geophysical*  
3 *Research: Atmospheres*, 110, D22S05, 10.1029/2005JD005935, 2005.
- 4 Swietlicki, E., Zhou, J., Berg, O. H., Martinsson, B. G., Frank, G., Cederfelt, S.-I., Dusek, U., Berner, A.,  
5 Birmili, W., Wiedensohler, A., Yuskiewicz, B., and Bower, K. N.: A closure study of sub-micrometer  
6 aerosol particle hygroscopic behaviour, *Atmospheric Research*, 50, 205-240, 10.1016/s0169-  
7 8095(98)00105-7, 1999.
- 8 Tang, I. N., and Munkelwitz, H. R.: Water activities, densities, and refractive indices of aqueous sulfates  
9 and sodium nitrate droplets of atmospheric importance, *J. Geophys. Res.*, 99, 18801-18808,  
10 10.1029/94jd01345, 1994.
- 11 Tuch, T. M., Haudek, A., Müller, T., Nowak, A., Wex, H., and Wiedensohler, A.: Design and  
12 performance of an automatic regenerating adsorption aerosol dryer for continuous operation at monitoring  
13 sites, *Atmos. Meas. Tech.*, 2, 417-422, 2009.
- 14 Varutbangkul, V., Brechtel, F. J., Bahreini, R., Ng, N. L., Keywood, M. D., Kroll, J. H., Flagan, R. C.,  
15 Seinfeld, J. H., Lee, A., and Goldstein, A. H.: Hygroscopicity of secondary organic aerosols formed by  
16 oxidation of cycloalkenes, monoterpenes, sesquiterpenes, and related compounds, *Atmos. Chem. Phys.*, 6,  
17 2367-2388, 10.5194/acp-6-2367-2006, 2006.
- 18 Virkkula, A., Van Dingenen, R., Raes, F., and Hjorth, J.: Hygroscopic properties of aerosol formed by  
19 oxidation of limonene,  $\alpha$ -pinene, and  $\beta$ -pinene, *J. Geophys. Res.*, 104, 3569-3579, 10.1029/1998jd100017,  
20 1999.
- 21 Wang, L., Khalizov, A. F., Zheng, J., Xu, W., Ma, Y., Lal, V., and Zhang, R.: Atmospheric nanoparticles  
22 formed from heterogeneous reactions of organics, *Nature Geosci.*, 3, 238-242,  
23 [http://www.nature.com/ngeo/journal/v3/n4/supinfo/ngeo778\\_S1.html](http://www.nature.com/ngeo/journal/v3/n4/supinfo/ngeo778_S1.html), 2010.
- 24 Wang, M., and Penner, J. E.: Aerosol indirect forcing in a global model with particle nucleation, *Atmos.*  
25 *Chem. Phys.*, 9, 239-260, 10.5194/acp-9-239-2009, 2009.
- 26 Weber, R. J., Marti, J. J., McMurry, P. H., Eisele, F. L., Tanner, D. J., and Jefferson, A.: Measurements of  
27 new particle formation and ultrafine particle growth rates at a clean continental site, *Journal of*  
28 *Geophysical Research: Atmospheres*, 102, 4375-4385, 10.1029/96JD03656, 1997.
- 29 Westervelt, D. M., Pierce, J. R., and Adams, P. J.: Analysis of feedbacks between nucleation rate, survival  
30 probability and cloud condensation nuclei formation, *Atmos. Chem. Phys.*, 14, 5577-5597, 10.5194/acp-  
31 14-5577-2014, 2014.
- 32 Wex, H., Petters, M. D., Carrico, C. M., Hallbauer, E., Massling, A., McMeeking, G. R., Poulain, L., Wu,  
33 Z., Kreidenweis, S. M., and Stratmann, F.: Towards closing the gap between hygroscopic growth and  
34 activation for secondary organic aerosol: Part 1 – Evidence from measurements, *Atmos. Chem. Phys.*, 9,  
35 3987-3997, 10.5194/acp-9-3987-2009, 2009.

- 1 Wiedensohler, A., Cheng, Y. F., Nowak, A., Wehner, B., Achtert, P., Berghof, M., Birmili, W., Wu, Z. J.,  
2 Hu, M., Zhu, T., Takegawa, N., Kita, K., Kondo, Y., Lou, S. R., Hofzumahaus, A., Holland, F., Wahner,  
3 A., Gunthe, S. S., Rose, D., Su, H., and Pöschl, U.: Rapid aerosol particle growth and increase of cloud  
4 condensation nucleus activity by secondary aerosol formation and condensation: A case study for regional  
5 air pollution in northeastern China, *J. Geophys. Res.*, 114, D00G08, 10.1029/2008jd010884, 2009.
- 6 Wiedensohler, A., Birmili, W., Nowak, A., Sonntag, A., Weinhold, K., Merkel, M., Wehner, B., Tuch, T.,  
7 Pfeifer, S., Fiebig, M., Fjaraa, A. M., Asmi, E., Sellegri, K., Depuy, R., Venzac, H., Villani, P., Laj, P.,  
8 Aalto, P., Ogren, J. A., Swietlicki, E., Williams, P., Roldin, P., Quincey, P., Hüglin, C., Fierz-  
9 Schmidhauser, R., Gysel, M., Weingartner, E., Riccobono, F., Santos, S., Gruning, C., Faloon, K.,  
10 Beddows, D., Harrison, R. M., Monahan, C., Jennings, S. G., O'Dowd, C. D., Marinoni, A., Horn, H. G.,  
11 Keck, L., Jiang, J., Scheckman, J., McMurry, P. H., Deng, Z., Zhao, C. S., Moerman, M., Henzing, B., de  
12 Leeuw, G., Loschau, G., and Bastian, S.: Mobility particle size spectrometers: harmonization of technical  
13 standards and data structure to facilitate high quality long-term observations of atmospheric particle  
14 number size distributions, *Atmos. Meas. Tech.*, 5, 657-685, DOI 10.5194/amt-5-657-2012, 2012.
- 15 Wu, Z. J., Nowak, A., Poulain, L., Herrmann, H., and Wiedensohler, A.: Hygroscopic behavior of  
16 atmospherically relevant water-soluble carboxylic salts and their influence on the water uptake of  
17 ammonium sulfate, *Atmos. Chem. Phys.*, 11, 12617-12626, 10.5194/acp-11-12617-2011, 2011.
- 18 Wu, Z. J., Poulain, L., Henning, S., Dieckmann, K., Birmili, W., Merkel, M., van Pinxteren, D., Spindler,  
19 G., Mueller, K., Stratmann, F., Herrmann, H., and Wiedensohler, A.: Relating particle hygroscopicity and  
20 CCN activity to chemical composition during the HCCT-2010 field campaign, *Atmospheric Chemistry  
21 and Physics*, 13, 7983-7996, 10.5194/acp-13-7983-2013, 2013.
- 22 Yue, D. L., Hu, M., Zhang, R. Y., Wang, Z. B., Zheng, J., Wu, Z. J., Wiedensohler, A., He, L. Y., Huang,  
23 X. F., and Zhu, T.: The roles of sulfuric acid in new particle formation and growth in the mega-city of  
24 Beijing, *Atmos. Chem. Phys.*, 10, 4953-4960, DOI 10.5194/acp-10-4953-2010, 2010.
- 25 Yue, D. L., Hu, M., Zhang, R. Y., Wu, Z. J., Su, H., Wang, Z. B., Peng, J. F., He, L. Y., Huang, X. F.,  
26 Gong, Y. G., and Wiedensohler, A.: Potential contribution of new particle formation to cloud  
27 condensation nuclei in Beijing, *Atmospheric Environment*, 45, 6070-6077,  
28 <http://dx.doi.org/10.1016/j.atmosenv.2011.07.037>, 2011.
- 29 Zdanovskii, B.: Novyi Metod Rascheta Rastvorimostei Elektrolitov v Mnogokomponentnykh Sistema, ,  
30 *Zh. Fiz. Khim*+, 22, 1478-1485, 1486-1495, 1948.
- 31 Zhang, Q., Stanier, C. O., Canagaratna, M. R., Jayne, J. T., Worsnop, D. R., Pandis, S. N., and Jimenez, J.  
32 L.: Insights into the Chemistry of New Particle Formation and Growth Events in Pittsburgh Based on  
33 Aerosol Mass Spectrometry, *Environmental Science & Technology*, 38, 4797-4809, 10.1021/es035417u,  
34 2004a.
- 35 Zhang, R., Suh, I., Zhao, J., Zhang, D., Fortner, E. C., Tie, X., Molina, L. T., and Molina, M. J.:  
36 Atmospheric New Particle Formation Enhanced by Organic Acids, *Science*, 304, 1487-1490,  
37 10.1126/science.1095139, 2004b.

Zhu, Y., Hinds, W. C., Kim, S., and Sioutas, C.: Concentration and Size Distribution of Ultrafine  
Particles Near a Major Highway, Journal of the Air & Waste Management Association, 52, 1032-1042,  
10.1080/10473289.2002.10470842, 2002.



## Tables and figures

Table 1: The summary of instruments and parameters used in this study.

Instrument	Parameter
TDMPS	Particle number size distribution
H-TDMA	Particle hygroscopicity
HR-ToF-AMS	Size-resolved chemical composition
Monitor – APSA 360 Horiba Europe	SO <sub>2</sub> concentration
Kipp & Zonen CM6 Pyranometer	Global solar irradiance

Table 2: Gravimetric densities  $\rho$  and hygroscopicity parameters  $\kappa$ .

Species	NH <sub>4</sub> NO <sub>3</sub>	H <sub>2</sub> SO <sub>4</sub>	NH <sub>4</sub> HSO <sub>4</sub>	(NH <sub>4</sub> ) <sub>2</sub> SO <sub>4</sub>	Organic matter
$\rho$ [kg/m <sup>3</sup> ]	1720	1830	1780	1769	1400
$\kappa$	0.67	0.92	0.61	0.61	0.1

Table 3: The water soluble fraction of newly formed particles and the ratios of H<sub>2</sub>SO<sub>4</sub> condensational growth to the observed particle growth

Dp	35 nm		50 nm		75 nm	
Date	$\epsilon$	$F_{GR_{H_2SO_4}}^*$	$\epsilon$	$F_{GR_{H_2SO_4}}$	$\epsilon$	$F_{GR_{H_2SO_4}}$
05-06-2008	--		24%	23%	20%	15%
06-06-2008	25%	23%	14%	17%	10%	11%
07-06-2008	34%	30%	23%	20%	17%	13%

\*  $F_{GR_{H_2SO_4}} = GR_{H_2SO_4} / GR_{obs}$ : The ratio of H<sub>2</sub>SO<sub>4</sub> condensational growth to the observed particle growth. Here, GR<sub>obs</sub> for 35, 50, and 75 nm were calculated over the time period during which Dm of log-normal ultrafine particle mode grew to 35, 50, and 75 nm, respectively, as indicated by the white circles in the Fig.1 (a).

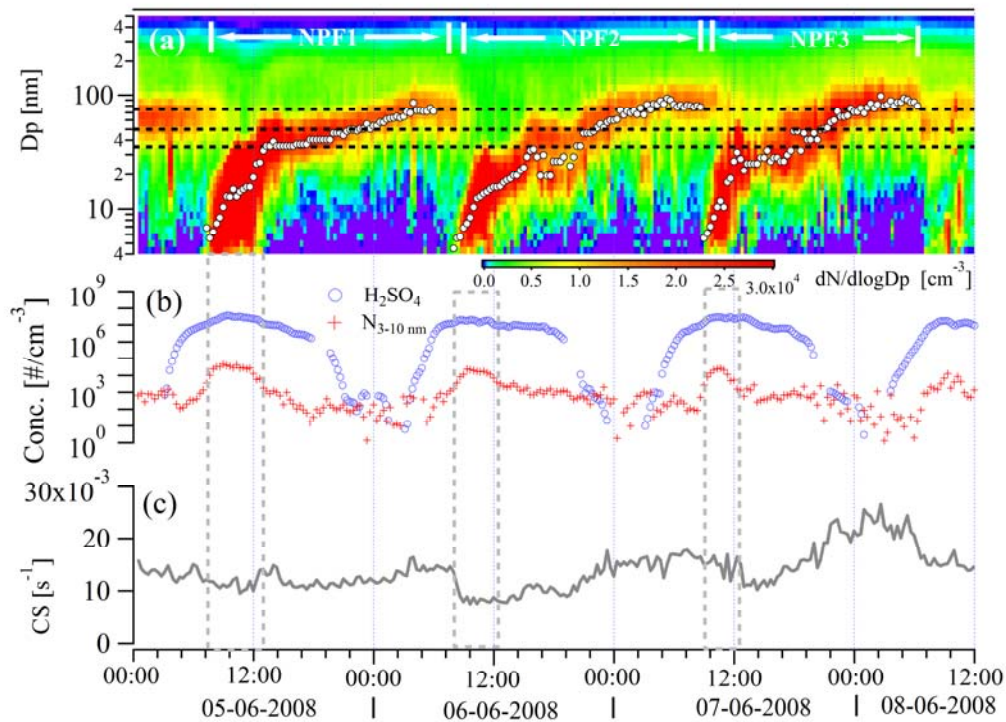


Fig. 1: Particle number size distribution (a), 3-10 nm particle number concentration and  $\text{H}_2\text{SO}_4$  concentration (b), condensation sink (CS) (c) during the NPF events. The starting and ending time of the events were marked in the upper place of panel (a) by NPF1, NPF2, and NPF3. The white circles in the panel (a) are the  $D_m$  of new particles modes. The grey dashed lines indicated the time period of particle formation. The black dashed lines in panel (a) indicate the particle sizes of 35, 50, and 75 nm. In the panel (b), the particle number concentration and  $\text{H}_2\text{SO}_4$  concentration share the same y axis and the unit.

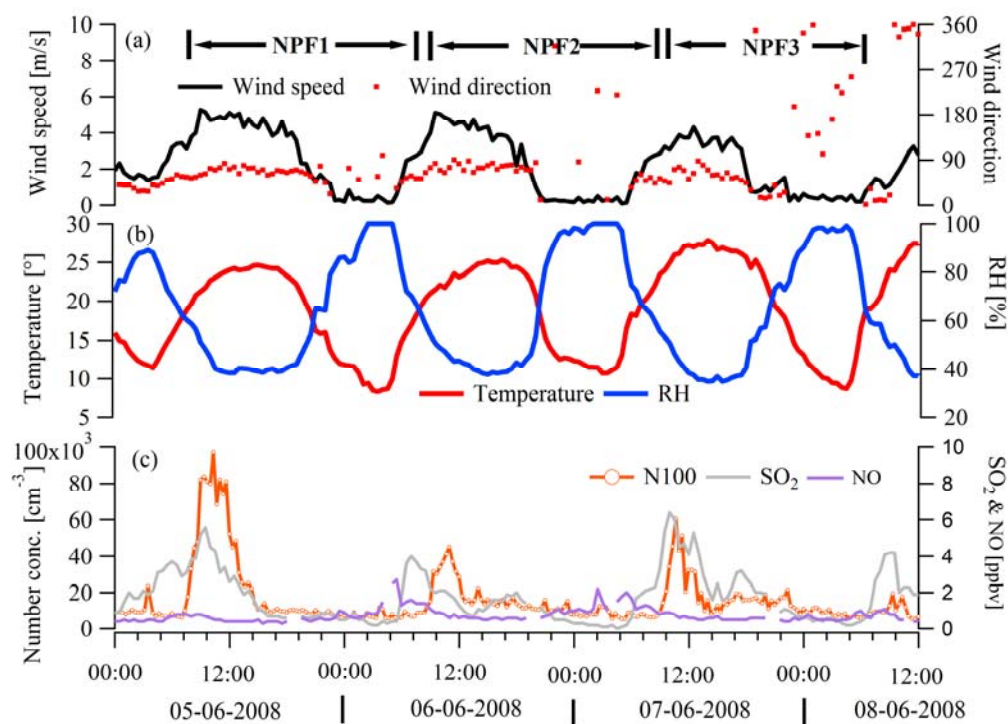
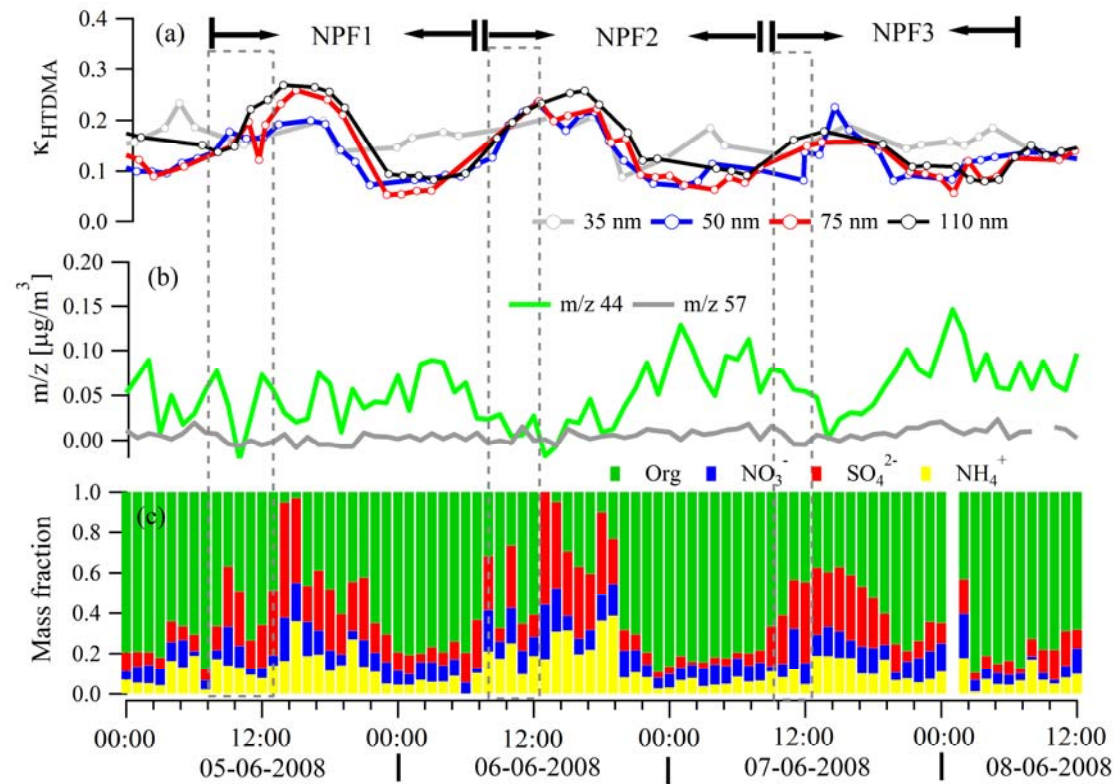


Fig. 2: The time series of wind speed and wind direction (a), ambient temperature and RH (b), and  $\text{SO}_2$  & NO concentrations and number concentrations of particles in diameters of 3-100 nm (c). The starting and ending time of the events were marked in the upper place of panel (a) by NPF1, NPF2, and NPF3.

1



2

3 Fig.3: Size-resolved particle hygroscopicity (a),  $m/z$  44 and 57 mass concentrations in 30-100 nm  
 4 particles (b), and mass fraction of organic, sulfate, nitrate, and ammonium in 30-100 nm particles (c). The  
 5 grey dashed lines indicated the time period of particle formation.

6

7

8

9

10

11

12

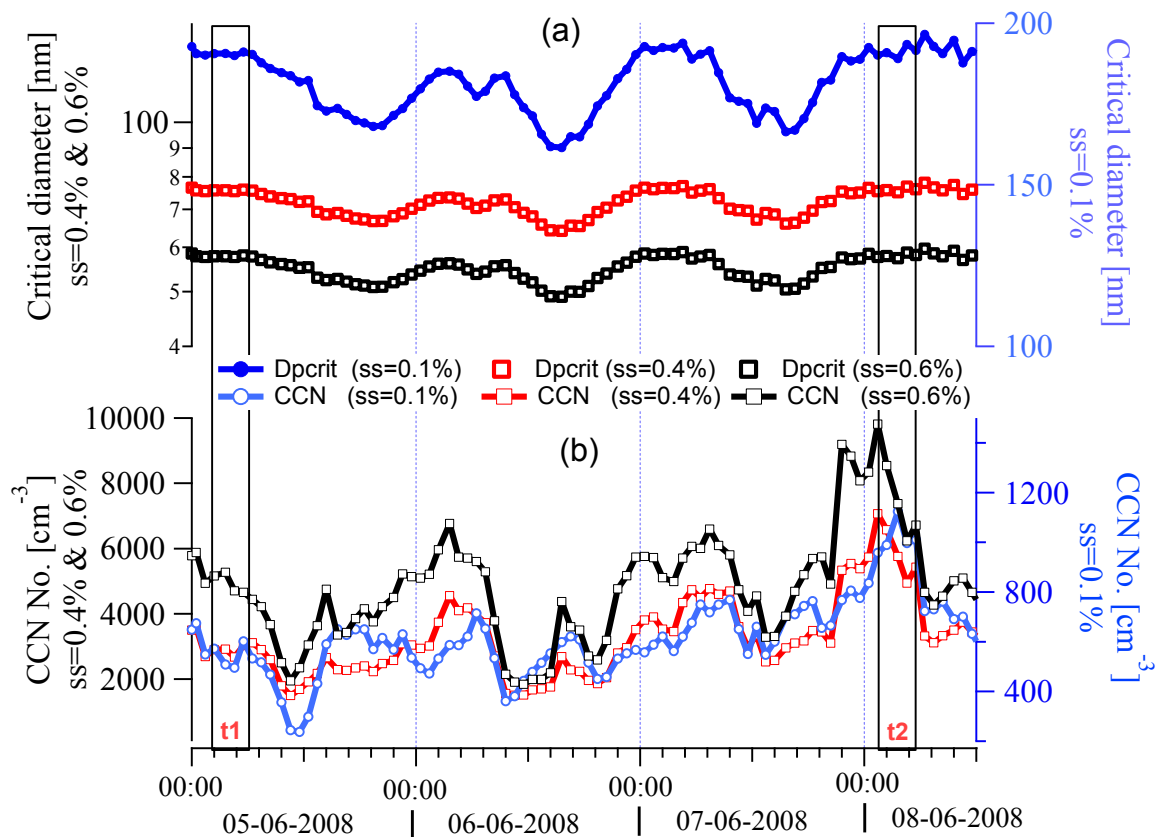


Fig. 4: Critical diameter (Dpcrit) and CCN number concentration during NPF events.